Austrian Journal of Earth Sciences | Volume 102 | 146 - 158 | Vienna | 2009

Last glaciation of the Šara Range (Balkan peninsula): Increasing dryness from the LGM to the Holocene

Joachim KUHLEMANN[1)2)*)], Milovan MILIVOJEVIĆ[3)], Ingrid KRUMREI[2)] & Peter W. KUBIK[4)]

[1)] Swiss Nuclear Safety Inspectorate ENSI, CH-5232 Villigen-ENSI, Switzerland.

[2)] Institute for Geosciences, University of Tübingen, D-72076 Tübingen, Sigwartstr. 10, Germany.

[3)] Geographical Institute ''Jovan Cvijić'', Serbian Academy of Sciences and Arts, Belgrade, Serbia.

[4)] Laboratory of Ion Beam Physics, ETH Zurich, CH-8093 Zurich, Switzerland.

[*)] Corresponding author, kuj@ensi.ch

KEYWORDS

Šara Range
Pleistocene
glaciation
Wuermian
LGM
ELA

Abstract

Based on field investigations, we have mapped the extent of moraines in the Šara Range (Balkan peninsula) in order to reconstruct the altitude of the glacier equilibrium line (ELA) during the Last Glacial Maximum (LGM) and successive glacier advances. The age of moraine stabilisation was determined by ^{10}Be exposure dating. With increasing altitude, late glacial and Holocene glacial depressions have been progressively filled with apparently inactive block glaciers in northerly exposure, indicating increasing seasonal dryness in more continental climate since the LGM. In southerly aspect, block glacier debris is rare and glacial cirques are poorly developed. The ELA during the LGM ranged between 1900 and 2000 m in NW to NE aspect, and 2100 to 2300 m in southerly aspect. The ELA of the Oldest Dryas is found 300 m higher in northerly aspect, and the ELA of the Younger Dryas about 50 m higher than that of the Oldest Dryas. Holocene niche glacier deposits have been found in well-protected cirques of three northexposed valleys.

There was hardly any west-east gradient of the ELA within the Šara Range in the LGM but a minor decline by about 200 m towards the Albanian Alps in the west at about 42° northern latitude. The west-east gradient seems to have been roughly similar in the late glacial. Presently preserved niche glaciers in the Albanian Alps reflect a similar gradient of eastward decreasing winter precipitation, resulting from topographic barriers, matching the LGM gradient.

In contrast to the studied west-east section of the Balkan peninsula, its western continuation along 42° northern latitude in the LGM shows that the western Mediterranean basin was much stronger affected by climate change. Frequent winterly meridional circulation in the Mediterranean triggered polar air outbreaks into the western Mediterranean basin which caused transport of air masses from the Sahara and admixed wet polar and subtropical air masses to the southern Balkan peninsula and further north towards the Fennoscandian ice shield. Westerly advection of moisture in the study area, however, was remarkably stable since the LGM, despite for strong temperature changes.

Die Ausdehnung von Moränen im Šara-Gebirge (Balkanhalbinsel) wurde kartiert, um die Höhenlage der Gletschergleichgewichtslinien (ELA) im Letzten Glazialen Maximum (LGM) und während nachfolgender Gletschervorstösse zu rekonstruieren. Deren Stabilisierungsalter wurde mit Hilfe von ^{10}Be-Expositionsdatierung bestimmt. Mit zunehmender Höhe wurden die in nördlicher Exposition gelegenen glazigenen Tröge fortschreitend von, heute scheinbar inaktiven, Blockgletschern verfüllt, was auf zunehmende saisonale Trockenheit im regional kontinentaleren Klima nach dem LGM hindeutet. In südlicher Exposition ist Blockgletschermaterial eher selten und Kar-Formen sind schlecht entwickelt. Die ELA lag im LGM in NW bis NE Exposition bei 1900 bis 2000 m und in südlicher Exposition bei 2100 bis 2300 m. Die ELA in Nordexposition lag in der Ältesten Dryaszeit vor ca. 15000 Jahren ca. 300 m höher als im LGM, und in der Jüngeren Dryaszeit nochmals 50 m höher. Ablagerungen holozäner Nischergletscher wurden in drei nordexponierten Gipfelkaren gefunden.

Im LGM ist innerhalb des Šara-Gebirges kein West-Ost-Gradient der ELA festzustellen. Auf dem 42. Breitengrad nach Westen sinkt die ELA im LGM in die Albanischen Alpen (Prokletje) um ca. 200 m ab. Dieser West-Gradient besteht im Spätglazial fort. Aktuell noch vorhandene Nischengletscher in den Albanischen Alpen spiegeln einen ähnlichen rezenten Gradienten von ostwärts abnehmenden Niederschlägen wider, der ähnlich wie im LGM durch die topographischer Barrieren hervorgerufen wird.

Im Kontrast zum West-Ost-Schnitt durch die Balkanhalbinsel zeigt die westliche Verlängerung am 42. Breitengrad, daß die ELA im westlichen Mittelmeerbecken wesentlich stärker vom Klimawandel betroffen war. Regelmäßige meridionale Zirkulation im Winterhalbjahr bewirkte ein Ausbrechen von Polarluft in das westliche Mittelmeerbecken, was eine ausgleichenden Luftmassenbewegung von der Sahara und gemischter polarer und subtropischer Luftmassen zur südlichen Balkanhalbinsel und weiter nordwärts zum Fennoskandischen Eisschild zur Folge hatte. Feuchteadvektion aus Westen in das Arbeitsgebiet hinein war seit dem LGM trotz der starken Temperaturveränderungen bemerkenswert stabil.

1. Introduction

Studies of mountain climate and ecology have become a major target in Europe, especially for circum-Mediterranean regions (IPCC report, Solomon et al., 2007). In the light of increasing aridity and temperatures expected for already dry

parts of Europe, discrimination of natural and man-made climate change is a major future issue (Luterbacher et al., 2005). This is particularly true for the regional water supply for intramontane depressions in the Balkan peninsula, especially in northern Macedonia which is presently supplied from the Šara Range. It is generally accepted that a better understanding of the climate system and its natural variability in the past provides key evidence for forecasts of near-future evolution. Mountain climate reconstructions in the geological past provide evidence of atmospheric processes at mid-tropospheric altitudes (e.g., Kuhlemann et al., 2008). An increasing spatial coverage of palaeoclimate evidence of circum-Mediterranean mountains is available from the limits of maximum glacier expansion during cold spells. A semi-continental scale proxy-data coverage is essential to validate coupled ocean-atmosphere circulation models of higher resolution (e.g. Jost et al., 2005).

Figure 1: Sketch map of southeastern Europe with the location of the study area.

For a better understanding of regional climatic response to rapid climate change during cold spells, particularly moisture transport, the Last Glacial Maximum (LGM) represents the best studied time slice. Numerous studies on fast changes of marine climate are available for the North Atlantic ocean, and recent studies in the north-western Mediterranean have demonstrated a causal link and immediate response of sea surface temperature (SST) and Greenland temperatures (Cacho et al., 2001, 2002; Meland et al., 2005). It has been shown that cold spells in the Mediterranean have been related to meltwater breakouts in the North Atlantic Ocean (Heinrich events). Dramatic short-term cooling especially affected the western Mediterranean basin, whereas southeastern Europe was much less affected (Hayes et al., 2005; Kuhlemann et al., 2008). Preferential north-directed flow of subtropical air over the Aegean Sea as a compensation of south-directed flow of polar air in the western Mediterranean basin is proposed as typical winterly mode of mid-tropospheric circulation (Kuhlemann et al., 2008). In this case, the target area, located within south-eastern Europe (Fig. 1), should have been characterised by a relatively high climatic snowline (better: equilibrium line altitude, ELA) during the LGM, and a mixture of southerly and westerly moisture supply, the latter being modulated by relatively low relief between the southern Adriatic Sea, northern Albania, forming a funneling gate from west to east.

In the continental scale of LGM climate, blocking of westerly moisture supply by central European high pressure raises the question to which degree the Fennoscandian ice shield was supplied from the south. Florineth and Schlüchter (1998, 2000) assume moisture supply along a cyclone track from the southwestern Mediterranean basin across central Italy and Pannonian basin to the N (Fig.2). Lake levels during the LGM, however, indicate relatively wet conditions in southern Spain, Greece, and southern Turkey, whereas central Italy remained relatively dry (Harrison et al., 1996). The eastern part of the Eastern Alps and the western Pannonian Basin also remained relatively dry (van Husen, 1997). According to modern polar cyclone tracks in the Mediterranean, an eastward continuation of cyclones across northern Albania and Kosovo area, or south of Greece and a subsequent turn to the N may be more likely for a moisture supply of the southern Fennoscandian ice shield.

It is evident that for constraining atmospheric flow in the LGM a stratigraphic framework for the mountains of southeastern Europe is essential, in order to trace moisture transport tracks. The west-east gradient of the ELA from the sou-

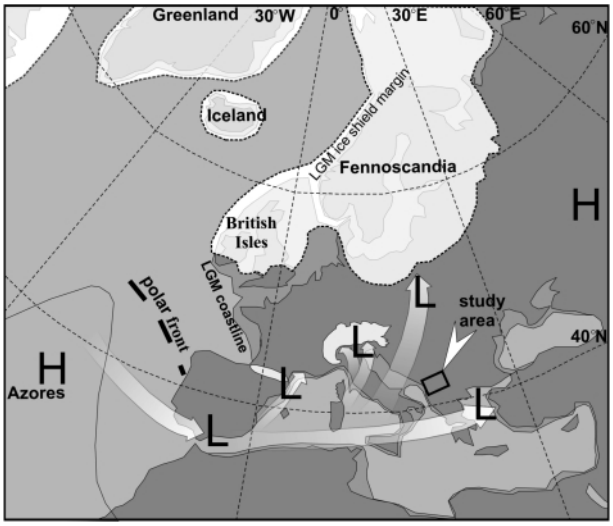

Figure 2: Preferred Mediterranean cyclone tracks during the Last Glacial Maximum according to Florineth and Schlüchter (2000). The outline of the Fennoscandian Iceshield is adopted from Svendsen et al. (2004).

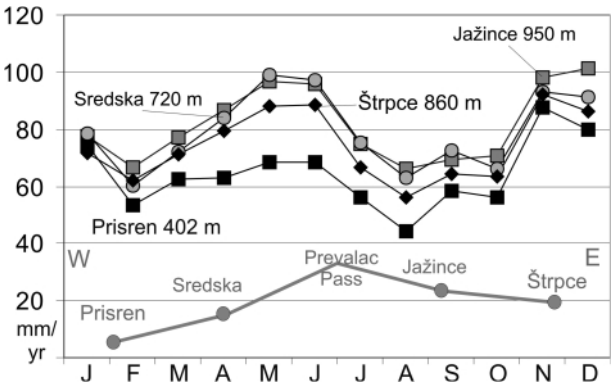

Figure 3: Monthly averages of precipitation along the Šara range (after Ocokoljić et al., 1994).

thern Adriatic to the east across northern Albania in the LGM and the late glacial allows constraining changes in an area where superimposed continental-scale atmospheric circulation was modified by relief. The aim of this paper is to track the regional W-E gradient of moisture supply by mapping of the ELA in the LGM and the late glacial.

2. Regional Setting

The Šara Range is located at the northern border of the Former Yugoslavian Republic of Macedonia (FYROM, Fig. 1). The SSW-ENE trending range is about 50 km long. The eastern and central sections are up to 2651 m high and quite rugged above 1500 m. Glacial relief is well-developed above 1500 m on the northern flank. Towards the west, the rugged crest grades into a glacially modified, basically hilly palaeorelief, with moderately shallow cirques to the southeast and shallow cirques to the northwest. To the south, a deeply incised glacial valley separates this summit surface from the highest massif of FYROM, which is partly rugged and deeply dissected, but in which also a high-elevated palaeosurface is preserved in places. All highlands southward drop into a dry intramontane depression, situated between 450 to 550 m elevation.

In the Šara Range, most valleys are covered by mixed deciduous and evergreen forests. The treeline with spruce is altered by human activity, mainly livestock breeding and hay production. More recently, skiing installations have been set up. Climate conditions in the Šara Range are semi-continental. Moisture is typically advected from westerly directions.

Geologically, the Šara Range belongs to the Western Pelagonian Zone (Korab Zone) with a polymetamorphic metasedimentary sequence (Jacobshagen et al., 1986; Mountrakis et al., 1987), with Hercynian granitoid intrusions in its central part, in continuation with the same tectonic unit in Greece (Reischmann et al., 2001). Hence, quartz for exposure dating by cosmogenic ^{10}Be is present in parts of the range.

Distribution of glacial landforms has been mapped by Menković et al. (2004), summarising older literature. Their maps show consistent occurrence of 4 moraine ridges of proper preservation in the forested montane belt. A similar setting is described in the Central Apennines (Giraudi and Frezzotti, 1997) and in Corsica (Kuhlemann et al., 2008). Towards the western part of this range, plateau-type glaciers had formed on a summit surface between 2200 and 2400 m during glacials (Menković et al., 2004). Further to the southwest, at the border to Albania on the northeastern flank of the Korab massif, a glacier tongue reached down to 1500 m (Menković et al., 2004).

In the present setting, precipitation increases from the northern foreland of the Šara Mountains towards the Korab foreland and further towards the west. Precipitation values from the Šara Mountains show two maxima in November/December and May/June, and a minimum in August (Ocokoljić et al., 1994). At the crest of the range, about 1300 mm/yr of precipitation is noted. A projection from the regional minimum elevation of 400 m at Prizren yields a vertical gradient of about 770 mm (+25 mm/100 m), calculated after data of Ocokoljić et al. (1994). There is no local west-east gradient observed between Prizren and Štrpce (Fig. 3). In the Albanian Alps, annual precipitation is much higher (Milivojević et al., 2008).

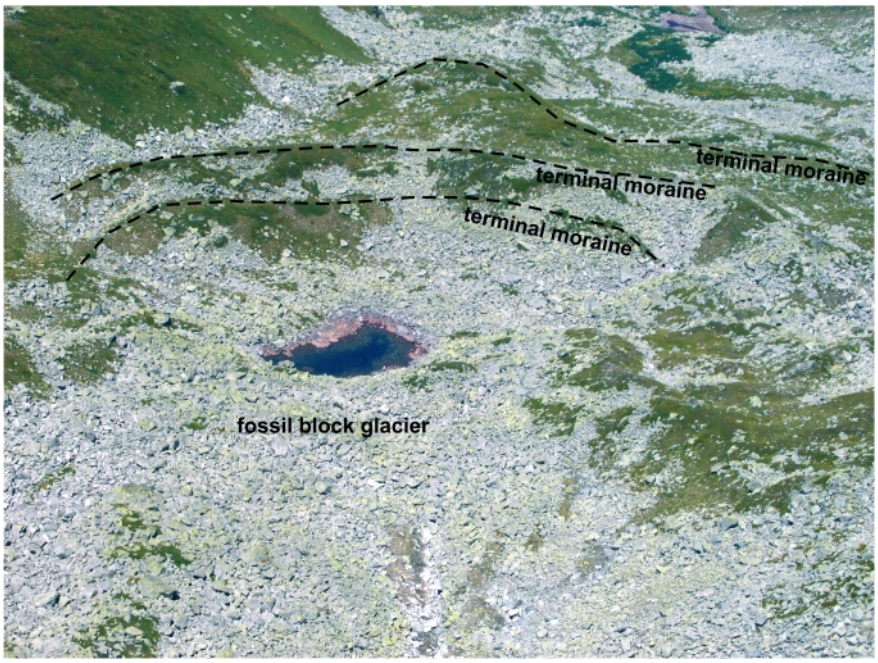

Figure 4: View from Jezerski Vrv (2586 m) into the NE-exposed cirque with Holocene moraines and block glacier accumulations (location in Fig. 5).

3. Analytical Methods

Exposure dating has been perfor-

med by analysing in situ-produced cosmogenic ^{10}Be in quartz of metamorphic rocks. Exposure dating is based on the assumption that rock surfaces like that of a glacial boulder are totally reset (at least 2 m of rock abraded) and exposed to cosmic rays ever since melting of glaciers. Chemical treatment of rock samples generally followed Kohl and Nishiizumi (1992) and von Blanckenburg et al. (2004). After optical evaluation and XRF control measurements of Al and trace element contents, purified quartz samples of up to 40 grams were prepared for Accelerator Mass Spectrometry (AMS) at ETH Zurich. The measured ^{10}Be/^{9}Be ratios were normalized to the standard S555 with a nominal value of 95.5 x 10^{-12} using a ^{10}Be half-life of 1.51 Ma.

^{10}Be exposure ages were calculated with the CRONUS-Earth online calculator version 2.1 (Balco et al., 2008) following the scaling scheme of Dunai (2000) and including a correction for the variation of the geomagnetic field in the past on the cosmogenic ^{10}Be production (Pigati and Lifton, 2004). Exposure ages of glacial boulders are corrected for topographic shielding, measured in the field. Elevation and latitude were determined from 1:50'000 topographic maps (Vojnogeografski Institut, 1985). The exposure ages are not corrected for cover of vegetation, snow or sediment, since in the mid-elevation sampling sites their effects are negligible. Postglacial weathering, depending on local climate and lithology with a certain range of error, has been considered for age calculation with 10 mm/ka as independent control of weathering rates is available from calc-alkaline granites of Corsica, exposed to similar precipitation rates (Kuhlemann et al., 2007). We have calculated the total 1σ error of our data.

The palaeotemperatures at higher elevations during cold glacial stages have been calculated by reconstruction of the equilibrium line altitude (ELA) on the base of the glacier margins, as constrained by trimlines and moraines. The size of the ablation area (1/3 to 1/2) relative to accumulation area (1/2 to 2/3) of a glacier (accumulation area ratio-method; AAR) is a good approximation of the ELA (Porter, 2001), but it depends on the hypsometry of the glacier surface and debris cover of the tongue. For a typical hypsometry of Wuermian glaciers, we chose an AAR of 0.67, according to moderately continental climate in the Carpathians (see Reuther et al., 2004, 2007). Potential errors of ELA estimates depend on the size and geometry of former glaciers, if their former outline is constrained by dated or correlated moraines. For small glaciers up to 3 km length, less than 1000 m of vertical range, having filled a single valley of typical Alpine hypsometry, the error is up to ±50 m. For larger glaciers and complex valley geometries, not relevant in the study region, the error is higher.

4. Field Evidence

We found a striking difference between a set of 4 latero-terminal moraines in the montane zone in northerly exposure and depositional features at higher altitude, above 1700 m. The moraine sets between 1600 and 1200 m altitude lack indications of block glacier activity. Below these moraines, only scarce scattered erratic boulders are found some 100 m lower in some valley floors. Above 1700 m altitude, block glacier deposits of impressive volume largely fill glacial depressions surrounded by latero-terminal moraines. The latero-terminal moraines above 1700 m comprise a lower one set of 3, rarely 4 ridges, and a higher set of 2, rarely 3 ridges, the latter frequently surrounding a glacial depression, occasionally filled with a lake. At subalpine elevations block glacier deposits dominate by far over moraine ridges (Fig.4). The latter are arranged around up to several hundreds of meters long shallow glacial depressions in the highest cirques of northerly exposition, now filled with block glacier deposits (Fig. 5). Angular meter-sized blocks, occasionally 10 m large, are filling the valley bottoms. The mounting of blocks is stable, and unlike moraines with angular blocks above 2000 m there is hardly matrix or soil found. These deposits have minor hill slopes and locally include depressions. Surprisingly, several water-filled ponds are present within such deposits. In one case, the water in such a pond was found to be about 10°C warm in late July 2007 which makes subsurface sealing by relict ice highly unlikely. More likely, such ponds are underlain by basal moraine and self-sealing fine-grained lake sediments.

Even in the highest cirques, angular blocks in block glacier deposits are covered by up to 10 cm-large yellow lichens of Rhizocarpon geographica and other lichen types. This indicates that their movement came to a halt several centuries ago in most places. There is however one exception in a cirque with less steep slopes, no rock walls, boulders of small to

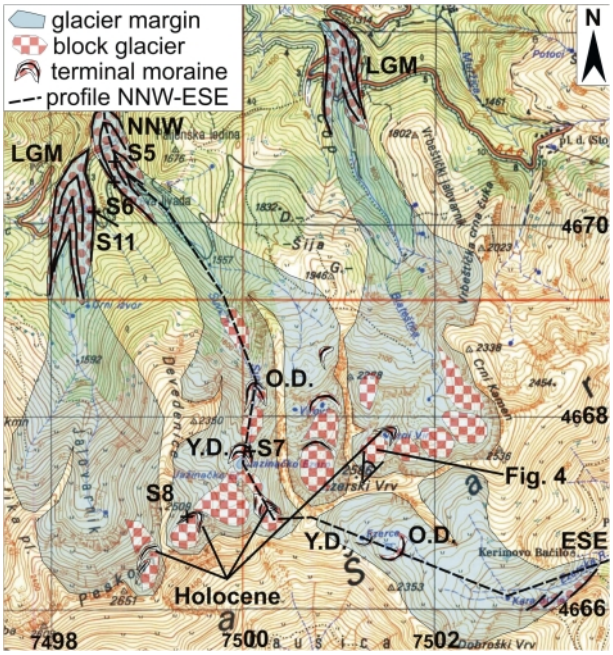

Figure 5: Local sketch map of the central Šara section with glacier deposits of the Last Glacial Maximum (LGM), the Oldest Dryas (O.D.), the Younger Dryas (Y.D.) and sampling sites (location in Fig. 6). The map scale is 1:50,000, coordinates represent the Gauss-Krüger system.

field code No.	lat. [°N]	long. [°E]	alt. [m]	Qz [g]	^{10}Be 10^4 [at g^{-1}]^a	topogr. shield.	sample thickn. [cm]	local prod. rate [at g^{-1} a^{-1}]	age (no erosion) [ka]^b	age (incl. erosion) [ka]^b
S5	42.18	20.98	1355	32.02	14.79±0.72	0.986	3	13.88	11.3±1.4	12.4±1.7
S6	42.18	20.98	1398	31.67	19.59±o.84	0.986	2	14.42	14.2±1.7	16.1±2.3
S7	42.16	21.00	2020	39.97	23.18±1.23	0.978	4	22.22	10.8±1.4	11.9±1.7
S8	42.15	20.99	2153	33.08	27.46±2.1	0.977	3	24.55	11.5±1.6	12.7±1.9
S11	42.17	20.98	1402	12.07	23.24±1.73	0.978	2	14.37	16.7±2.3	19.4±3.2
S13	42.14	20.99	2300	36.33	31.11±1.36	0.988	4	27.20	11.6±1.4	12.9±1.8
S16	42.01	20.79	2212	39.20	32.95±1.64	0.991	4	25.63	13.1±1.6	14.7±2.1
S18	42.74	20.82	1776	30.93	23.73±1.27	0.996	3	19.14	12.9±1.6	14.4±2.1

a 1σ uncertainty indicates the AMS measurement uncertainty
b 1σ uncertainty includes the uncertainties in the spallogenic SLHL nuclide production rate and the nuclide production rate by muons

Table 1: Exposure ages and relevant data for calculation of all samples.

moderate size, and more fine-grained material than elsewhere on the northern flank of the Šara Range. In the flat cirque bottom, several small flat moraine ridges were found, lacking boulders of proper size for dating. Situated higher than 2300 m a.s.l , 150 m above a set of moraines around a lakes at 2150 m, the innermost moraines are surrounding a swampy flat. The local setting suggests that this cirque hosted a niche glacier or a nivation hollow during coldest phases of the Holocene, possibly including the Little Ice Age. Two more cirques next to the west, situated below rock walls and filled with large boulders, also expose matrix-poor boulder ridges well above a depression filled with rock glacier deposits. A similar setting is found eastward in a SE-exposed cirque (Fig. 4). These boulder ridges represent lateral moraines. During the sampling campaign in late July 2007, few relict snow fields were preserved at the foot of the rock walls. In the beech forest zone next to the villages at altitudes below 1200 m a.s.l, isolated large erratic boulders are found, but no landforms reminding of moraines. These regions experienced a long history of anthropogenic overprint.

5. Exposure Ages

Samples have been taken where suitable terminal moraines contained large boulders of quartz-bearing rocks (Fig. 6). Samples have been taken from the mentioned 3 groups of moraine complexes. Boulders of sufficient size (>1.5 m above soil, stable position) are very rare and partly absent.

Four samples from the lowest and thus oldest moraine complex on the moist northerly slope of the Šara Range were measurable. Three of them were taken in beech forests on slopes with angles of 15 to 20 degrees. S5 and S6 represent the same moraine ridge. The obtained ages are younger than LGM, probably because the sampled boulders have been rotated within the matrix and moved downslope of the respective moraine. Only boulders on moraine crests were sampled which looked like being situated in a fairly stable position, or at least became stabilized more early than on the steeper moraine slopes. Sample S11 best fits proper sampling conditions as the moraine ridge had a slope of about 10 degrees. The data however confirm that a deposition of moraines happened in the LGM, as assumed already by Menković et al. (2004).

Sample S18 was taken at Karanikola Pass in the south-exposed southwestern part of the Range on a 10 degree slope of the inner

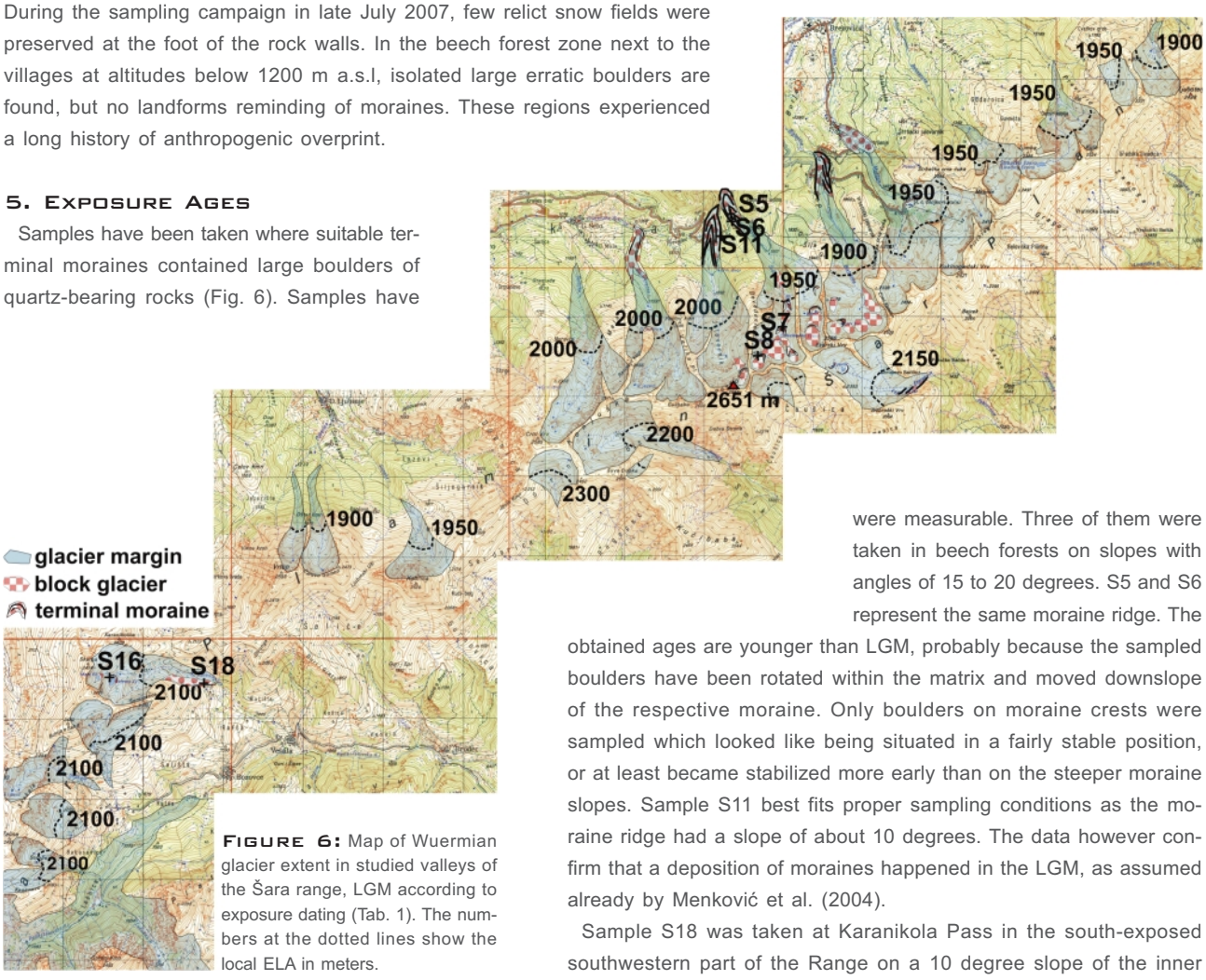

Figure 6: Map of Wuermian glacier extent in studied valleys of the Šara range, LGM according to exposure dating (Tab. 1). The numbers at the dotted lines show the local ELA in meters.

side of the moraine. Some movement and tilt is likely also for this sample. Moreover, the sampled schist boulder appeared to be strongly weathered and spallation from its top surface seems likely.

One sample from the middle moraine complex was measured at Karanikola Pass, surrounding the lower lake in this southeast-exposed cirque (S16). The 5 m large sampled boulder is situated in a matrix-poor moraine of low slope. It matches Oldest Dryas depositional age (Fig. 7).

One sample from the upper moraine complex was measured. Sample S8 represents the 2nd advance and thus the inner moraine ridge surrounding a lake of 1 ha size. The age of 12 ka confirms Younger Dryas deposition. The sampled boulder is placed on top of the terminal moraine ridge in point contact to almost matrix-free glacial boulders, unlikely to have been moved.

5.1 Discussion of exposure data

Exposure dating in this particular region is difficult because of uncertainties of age correction for rock weathering and air pressure. Rock weathering would reduce the apparent exposure ages, requiring correction (Tab. 1), and so would an air pressure of more than 1013 hPa. For air pressure, no independent control is available. Raw ages with zero erosion are obviously too young. This problem applies also to the other data sets of southeastern Europe, e.g. of Reuther et al. (2004) from the western end of the South Carpathians. These authors find typical LGM maximum glacier advances, expected between 24 and 18 ka, (in average 20 ka) to be centered at 16 ka.

To us, this apparent systematic underestimate of exposure ages, obtained by different groups and laboratories in a similar range, calls for a common natural explanation of special regional conditions. For a calculation of exposure ages, numerous assumptions are required which normally cannot be independently controlled. These assumptions include (a) weathering rates, (b) snow cover, (c) air pressure, as main uncertainties.

(a) Weathering rates are quite variable and range between 2 and 20 mm/ka for granite of different degree of micro-fracturing, post-tectonic cementation (chlorite, quartz), anortite/biotite-content, and climate (Kuhlemann et al., 2007). Minima were found at silicified aplite dykes. In settings of high precipitation (1300 to 1500 mm/a), a weathering rate of 15 mm/ka for LGM boulders was found to best fit to normal calc-alkaline granite boulders (Kuhlemann et al., 2008). In case of schists, weathering rates may exceed 20 mm/ka of weathering. Unfortunately, we have no independent constraints from the Šara Range.

(b) Air pressure should be included in exposure age calculation on the base of climate models of the past (GCM) although such results can hardly be validated with proxy-data. The western Russian high pressure cell had significant potential to affect the study region by high pressure in winter. If cold climate phases of the LIA were a useful analogue for cold phases since the LGM, the effect of air pressure on the study region was unimportant, following modelling results of Xoplaki et al. (2001).

(c) Snow cover in the past is virtually impossible to calculate. 30 to 40 cm of effective average annual water column significantly decrease exposure ages by shielding of cosmic rays. The problem increases with increasing elevation, at the sites of late glacial deposits are more affected than those of the LGM in the lower parts of the valleys. In the present set of samples, this correction cannot be performed for higher elevation sites. The potential effect for LGM moraines is assumed to be negligible.

In the light of increasing block glacier activity in the late glacial, periglacial movement of LGM moraine material seems likely. As a result, final consolidation of moraines probably lasted until 11.7 ka, and exposure ages of boulders reflect different degree of periglacial tilting.

If the above mentioned corrections of raw exposure ages and periglacial instability until 11.7 ka are accepted, the glacier advances between 1100 and 1500 m altitude are correla-

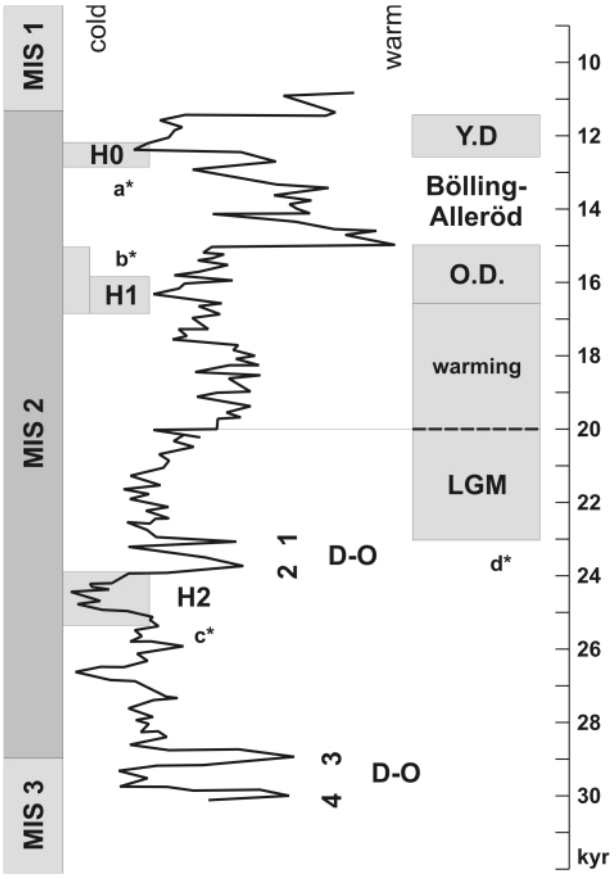

Figure 7: Presumed stratigraphic ages of glacial advances in the Šara range, correlated with the Greenland ice core record (Shackleton et al., 2004) and dated cold spells in the last 30 kyrs, namely Heinrich event H0 (a*, Severinghaus et al., 1998), initiating the Younger Dryas (Y.D.) cold phase at the end of the last glacial, Heinrich event H1 (b* Bond et al., 1997) initiating the Oldest Dryas (O.D.) cold phase, and Heinrich event H2 (c* Cacho et al., 2002), prior to the Last Glacial Maximum (LGM, d* Bard, 1999). Short warmings of the glacial correspond to Dansgaard-Oeschger-Events (D-O) 1 to 4.

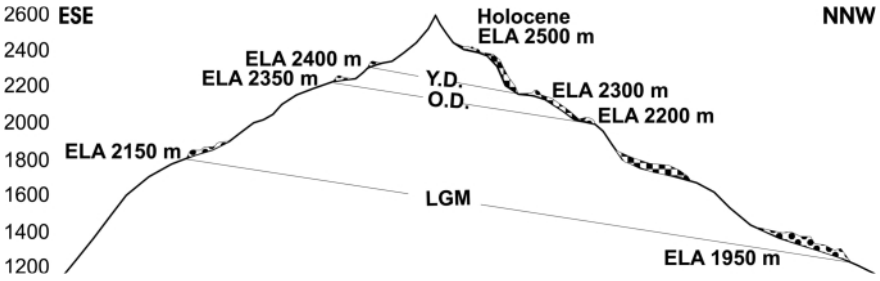

Figure 8: Schematic N-S cross section of the Šara range with terminal moraines.

ted with the LGM glacier advances, with lower altitudes on the northern slopes and higher altitudes on the southern slopes. Similarly, moraines at altitudes between 1600 and 2200 m are tentatively correlated with the Oldest Dryas, and moraines at altitudes between 2100 and 2400 m are tentatively correlated with the Younger Dryas. Small local moraines at higher elevation, close to the crest, are tentatively attributed to the well-known cold spell at 8.2 ka, triggered by the last meltwater breakout of the Laurentian ice shield into the North Atlantic Ocean (Bond et al., 1997).

6. Local climate implications

Especially in the case of higher and narrow cirques surrounded by steep rock walls, spatial arrangements indicate morphogenetic and morphochronologic relations between the moraines and rock glaciers. These geomorphic features constrain the evolution of the latest glaciers in the following succession: ablation complexes → debris covered glaciers, or black glaciers → ice-cored rock glaciers → debris rock glaciers or secondary rock glaciers. This succession is typical also in other mountain ranges of southeastern Europe, namely the South Carpathians (Urdea, 2004). In an increasingly continental climate this morphogenetic succession is typical. Since rock glacier deposits are lacking inside LGM latero-terminal moraines and below them, we conclude that climate was less continental in the LGM than lateron. Scattered erratic boulders below LGM moraines testify more extensive glaciation at an unknown time prior to the LGM, which is typical for the southern Balkan peninsula (Hughes et al., 2007; Hughes and Woodward, 2008).

As exposed in Fig. 6, the ELA in the LGM slighly varies on the northern flank of the range. The highest level is reached in the center (2000 m), whereas it slightly declines towards the west and east (1900 m). At the eastern end of the high range, light-coloured carbonate rocks probably contribute to local cooling. On the southern flank, the ELA is significantly higher, although the few valleys with glacial features are protected against insolation from the SW and potentially benefited from drift snow. Hence, an ELA of 2100 m is a minimum and 2300 m, such as found in an unprotected cirque, is more typical. A relatively high ELA contrast between the northern and southern flank of the Šara Range is explained by advection of heat produced in the intramontane depression south of the range during the warm season, similar as at present times.

The ELA of the Oldest Dryas is found at about 2200 m in northerly, and about 2300 m in two southeasterly-exposed valleys (Fig. 8). The latter cirques benefited from drift snow. Younger Dryas ELA is found 40 to 80 m higher up in the same valleys. As compared to the LGM, the ELA contrast between the north and south-exposed flanks, respectively, is decreasing upward and converges towards the crest. In schematic N-S cross section (Fig. 8), however, baselines connecting the moraine terminations of the respective stages all have the same slope. We interpret this constant slope of the baselines as to reflect similar direction of moisture advection during cold climate spells, preferentially from the west, similar to the present. Since winter precipitations rates increase towards the west, the ELA should decline in this direction.

Glacial retreat stages with well-preserved moraines and maximum advances in the Wuermian have been mapped by Milivojević et al. (2008) in the Albanian Alps, particularly Prokletije Mt. (eastern Montenegro and northern Albania) in northerly exposition. Different from the Šara Range, small niche glaciers are preserved in cirques at 2000 to 2200 m elevation, below steep limestone walls. Their existence is explained by microclimatic conditions, similar as in the case of the Debeli Namet glacier at Durmitor in the central Dinarides (Hughes, 2007), since the regional ELA is supposed to be higher than the peak level. Milivojević et al. (2008) found an ELA of 1750 m for the strongest, presumably Wuermian glacier advance, 1950 m ELA for the next recessional stage, and little higher than 2100 m for the last recessional stage. Hughes and Woodward (2008) provide U-series ages slightly younger than but probably prepresenting Younger Dryas depositional age 1 km down-valley of the recent limit of the Debeli Namet glacier. They note this as evidence of dryer climate conditions as compared to the LGM.

Assuming that the mapped Wuermian maximum glacier advance in Prokletije Mt. (undated) matches the dated LGM advance of the Šara Range, and that the two reces-

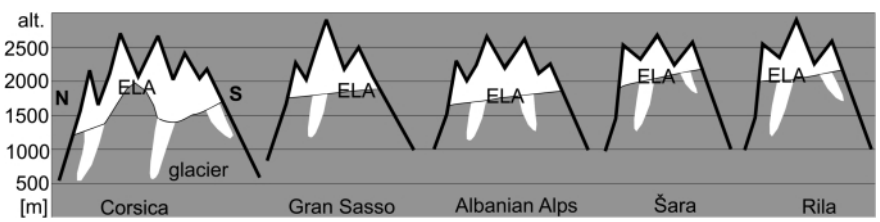

Figure 9: Schematic west-east section of ELA and glacier extent to low elevations along 42°N in the central Mediterranean.

sional stages 2 and 3 of Milivojević et al. (2008) match Oldest and Younger Dryas like in the Šara Range, and like in the Apennines (Giraudi and Frezzotti, 1997), the ELA in Prokletije (Albanian Alps) was lower by about 200 m during these 3 cold stages as compared to the Šara Range. This suggests a fairly constant west-east gradient of the ELA and hence of precipitation in the LGM between the Albanian Alps and the Šara Range at 42° northern latitude (Fig.9). Further to the east, the ELA in the Rila massif is about 100 m than in the Šara Range, with less contrast between southerly and northerly exposure (Kuhlemann et al., 2009). This indicates further eastward drying.in the LGM Further to the west at 42° northern latitude, the ELA in the Central Apennines (Giraudi and Frezzotti, 1997) is somewhat higher than in the Albanian Alps, but drops dramatically towards Corsica (Kuhlemann et al., 2008).

7. Mediterranean mountain climate during the LGM

A Mediterranean-wide compilation of the ELA of LGM glacier expansion has recently been updated by Kuhlemann et al. (2008). The Mediterranean ELA map (Fig. 10) is, particularly in southeastern Europe, still locally based on work compiled by Messerli (1967). The present paper, however, provides new regional field evidence and exposure ages for this region. Currently available ELA reconstructions for the maximum glaciation in Iberia, Italy, and the southern Dinarides (mainly Greece) partly lack precise chronology to pin it to the LGM, but for the Alps it is known that the maximum extent of glaciers occurred simultaneously with that of the northern hemisphere in the LGM (Florineth and Schlüchter, 1998). Nevertheless, in the northern Pyrenees, glaciers were less far extended during the LGM than during earlier phases in the last glacial cycle (García-Ruiz et al., 2003) and this seems to apply throughout Iberia (Alberti et al., 2004). In the western Southern Carpathians, evidence exists for a stronger advance earlier in the Wuermian as well (Reuther et al., 2007). In northern Greece, maximum glacier extent in the Wuermian occurred during the LGM (Boenzi and Palmentola, 1997; Woodward et al., 2004; Hughes et al., 2007). Older ELA maps for Greece and southern Italy show the maximum expansion in the last glacial cycle (Giraudi, 2004), not necessarily strictly within the LGM (Pérez Alberti et al., 2004). A map (Fig. 11) comparing the modern ELA with that of the LGM highlights strong changes of regional gradients but only moderate changes of the pattern (Kuhlemann et al., 2008, modified). Particularly in the region of interest, the southern Dinarides, the pattern apparently is quite constant and the two-dimensional ELA pattern fits the W-E gradient described here quite well. In map scale it is however evident that the Adriatic coast of Croatia is the key site of the Dinarides, where the ELA reached a regional minimum (Marjanac and Marjanac, 2004). This zone of maximum winter precipitation and cold extended towards Montenegro and Albania.

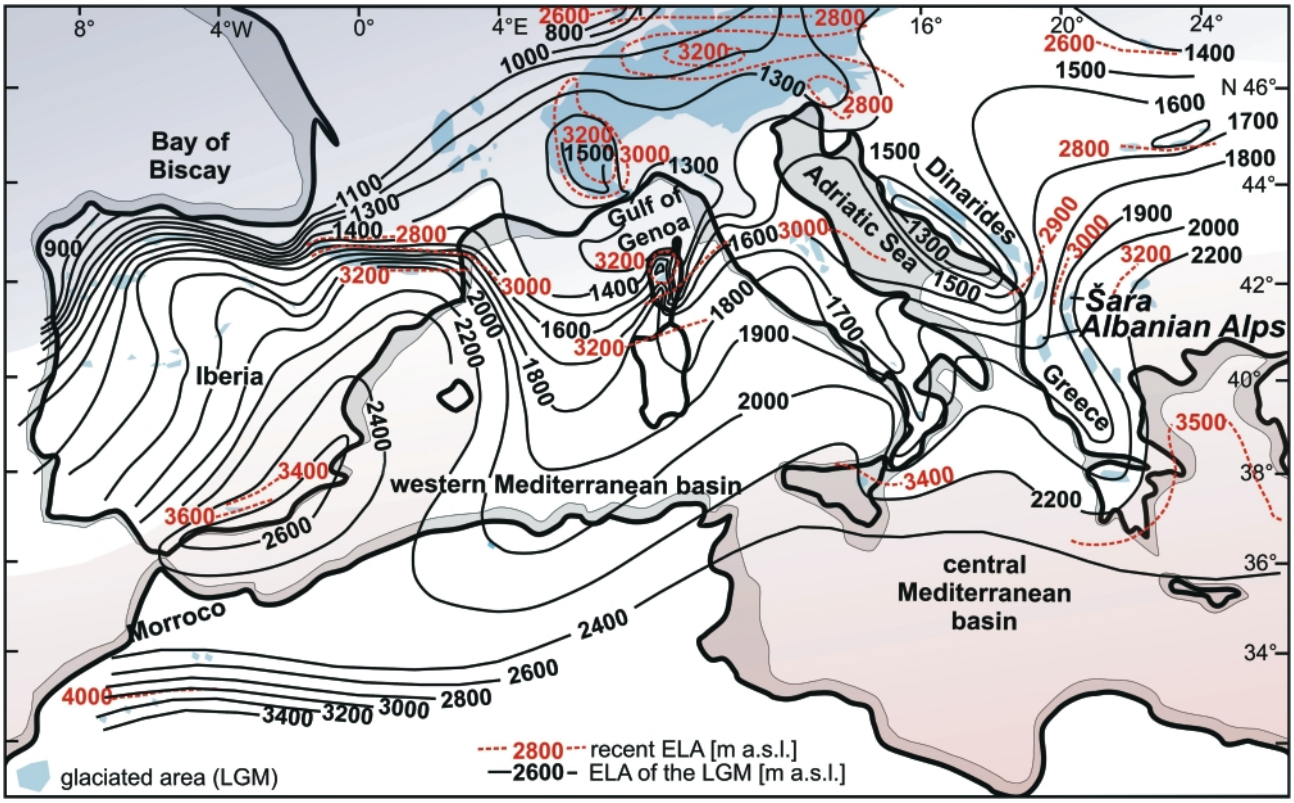

Figure 10: Mediterranean ELA of the LGM and the Present (modified from Kuhlemann et al., 2008, with references). The map indicates areas glaciated in the LGM and exposed shelf area (not to scale). Construction of ELA isolines for the LGM is partly based on undated Wuermian moraines which do not necessarily match the LGM. Red transparent colour towards the south and blue colour towards the north indicates a general temperature trend.

7.1 Scenario for atmospheric flow during LGM and the late glacial

We assume considerable cyclonic activity in the western Mediterranean during the LGM, but not a dominant zonal track of storms across the basin. Today, fast-moving Atlantic disturbances rush through the Mediterranean basin and cause moderate precipitation that increases with elevation. We suggest more frequent local cyclone generation in the Gulf of Genoa, particularly in winter and spring (Fig. 12), like during the winter 2008/2009. In the southern Balkan peninsula, LGM cyclone tracks may have followed modern tracks across and around southern Greece (Peleponnes) and across northern Albania and turned northward, triggered by the polar front. Such cyclone tracks, however, are typical for the southern Balkan peninsula in various modes of mid-tropospheric circulation, and they may be less specific as they are for the Alps and the northern Balkan peninsula. The proposed dominant winter circulation mode is certainly speculative and just one of several other possible scenarios, as can be learned from better constrained cold phases of the LIA (e.g., Xoplaki et al., 2001).

With an LGM polar front on average located further south (COHMAP, 1988), southeast-directed passage of polar front cyclones from the eastern Atlantic ocean and their perturbations into the Mediterranean would cause outbreaks of polar air into the Gulf of Lions (Fig. 9) more frequently than at Present (Kageyama et al., 2006). Frequent distinctly meridional circulation during cold seasons with high synoptic activity, as reflected by the LGM ELA pattern, may have alternated with zonal circulation and calm activity during warm seasons, which in the average of the LGM year may even have been the dominant mode, as inferred from the high-resolution climate model HadRM (Jost et al., 2005). Polar air masses invading the western Mediterranean basin typically pass through the funnel between the Alps and the Pyrenees (Rohling et al., 1998; Cacho et al., 2002). The Alps are forming the larger barrier, particularly when strongly glaciated in the LGM, and thus air masses breaking through the funnel diverged, preferentially turned left and frequently produced a cyclonal vortex in the rear of the Alps in the Gulf of Genoa. Cyclones born here then appear to have followed established tracks to the southeast, affecting the study region, and unusual tracks along the Adriatic coast and directly towards the Alps.

Meridional atmospheric flow would be favoured by a low pressure gradient between the Azores high and the Island low pressure cells, blocking zonal flow of the westerlies. The regional effect in western-central Europe was enhanced if interannual variation would have favoured a low pressure gradient in winter and a high pressure gradient in summer, similar to the LIA (Cassou et al., 2004). At present, a blocking N-directed high-pressure ridge between the Azores and Iceland triggers a roughly S-directed geostrophic flow of polar air on its

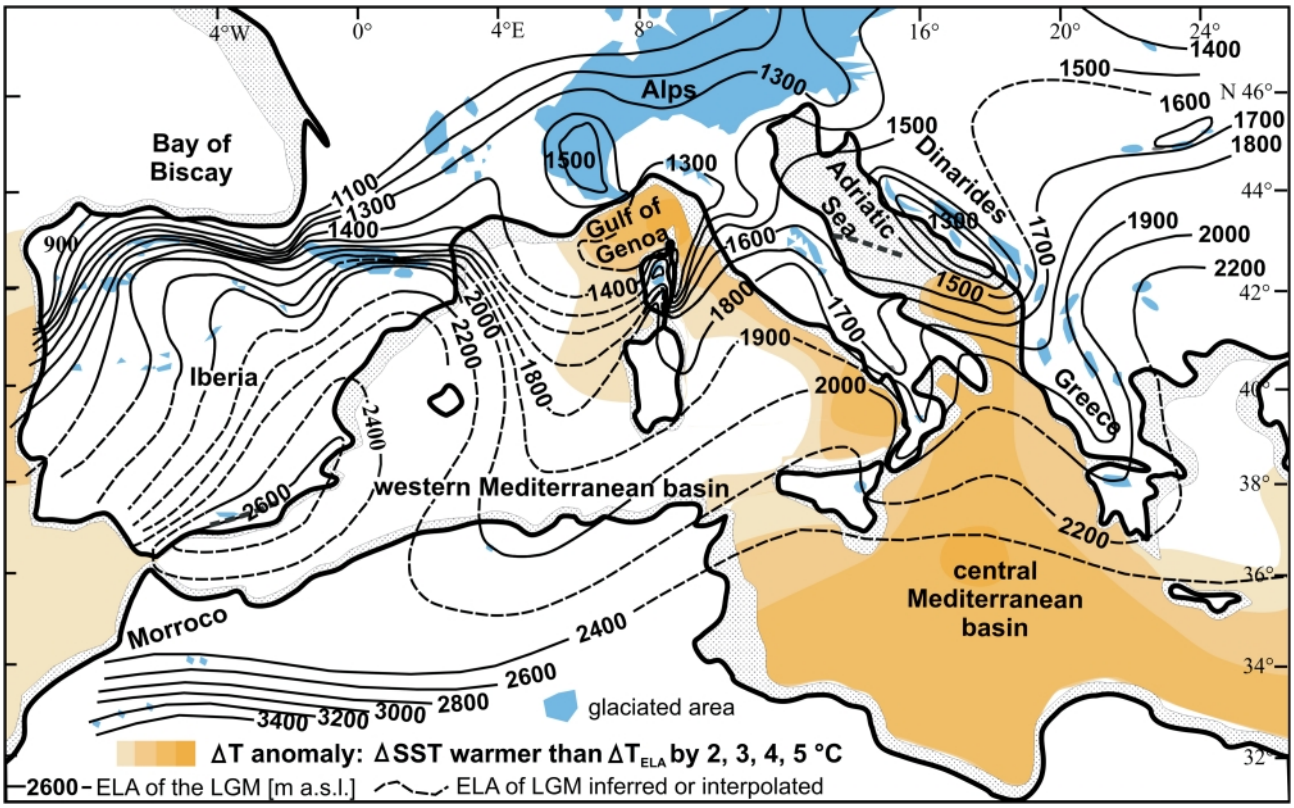

Figure 11: Mediterranean LGM warm SST anomalies driving local convection (Kuhlemann et al., 2008, modified). The colour coding of the sea shows anomalously high sea-surface temperatures as compared to the atmospheric temperature between 1500 and 3000 m altitude, as deduced from the ELA lowering, assuming a pure temperature effect (end member scenario). The higher the apparent temperature anomaly, the stronger would the steep lapse rate drive convection and hence local precipitation.

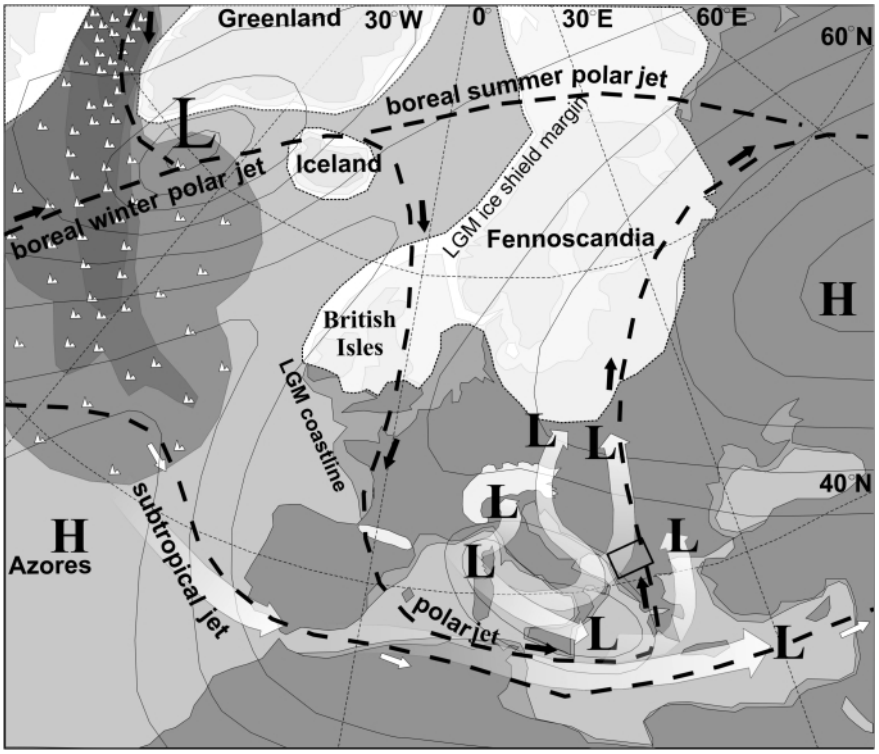

Figure 12: Sketch of the postulated typical winterly European atmospheric circulation in the LGM. Note that lines locating the subtropical and the polar jet stream shall reflect only a central line of a broad band of increased likelyhood. The meandering jet streams of the Rossby waves are highly mobile. Flow of polar air in the higher atmosphere is indicated by black arrows whereas white arrows indicate the flow of subtropical air masses. White transparent flow lines indicate preferential cyclone tracks. Note that the working area (black rectangle) is situated close to a northeast-trending cyclone track which would trigger south to southwest winds prior to cyclone passage and cold westerly winds in its rear. The locations of high and low pressure cells as well as the isoline pattern are tentative. Alternative proposals for better constrained cold spells of the Little Ice age are discussed by Xoplaki et al. (2001).

eastern flank into the western Mediterranean (Ω-setting). Such regional setting was more common in the late Little Ice Age than in the 20th century (Jacobeit et al., 2001). As a result, polar air invading northwestern Africa likely caused more dust storms and triggered cyclogenesis over the desert, as the polar jet came close to the subtropical jet stream. As a consequence, desert air probably moved towards the NE across the Aegean Sea, as indicated by the north-extending lobe of the ELA in southeastern Europe (Fig. 12). This is consistent with observations of enhanced wind-blown dust supply from the Sahara into the eastern Mediterranean during glacial times (Larrasoana et al., 2003). Above relatively warm Mediterranean waters of the central and eastern basin, these NE-directed desert air masses would have mixed with the invading convective polar air masses and picked up local moisture before moving northward. During cold spells of the late glacial, this type of mid-tropospheric circulation apparently became less frequent as compared to the LGM.

8. Conclusions

Comparison of the recent and ancient snowline during various cold spells, as preserved by moraines deposited during glacier advances, yields information of preferential moisture transport. In a representative cross-section of the central Šara Range, a typical insolation-controlled north-south gradient is observed for cold spells from the LGM to the LIA. The west-east gradient of winterly precipitation is virtually the same during cold spells, shown for the LGM, the Oldest and the Younger Dryas, and the Little Ice Age. This is much different from the western Mediterranean basin, which was much more affected by climate change. Frequent winterly meridional circulation in the Mediterranean triggered polar air outbreaks into the western Mediterranean basin which appear to have caused transport of admixed wet polar and subtropical air masses from the central Mediterranean basin and northwestern Africa across Greece to the north, supplying moisture to the Fennoscandian ice shield. Westerly advection of moisture in the study area, however, was remarkably stable since the LGM, despite for temperature changes. Hence, the study region appears to have been less strongly affected by climate change than the western Mediterranean.

Acknowledgements

We are grateful for diplomatic and logistic support of fieldwork in summer 2007 by Klaus Denecke (OSCE) and Rastko Nikolić in difficult times. Special thanks go to Klaus Schropp and his inspiring knowledge of flora, potential location of officially cleared landmines around Karanikola pass, and 2-wheel transport on rough roads. Local people supported field work and a helpful person from Belgrade utilised safe fast transport of samples to Tuebingen. Samples were processed by Dagmar Kost, Gerlinde Höckh and Dorothea Mühlbayer-Renner. Two very constructive and helpful anonymous reviews are gratefully acknowledged. This study has been funded by the German Science Foundation (DFG).

References

Alberti, A.P., Diaz, M.V. and Chao, R.B., 2004. Pleistocene glaciation in Spain. In: J. Ehlers and P.L. Gibbard (eds.), Quaternary Glaciations – Extent and chronology. Developments in Quaternary Sciences, 2, pp. 389-394.

Balco, G., Stone, J., Lifton, N. and Dunai, T., 2008. A complete and easily accessible means of calculating surface exposure ages or erosion rates from ^{10}Be and ^{26}Al measurements. Quaternary Geochronology, 3, 174-195.

Bard, E., 1999. PALEOCLIMATE: Ice Age Temperatures and Geochemistry. Science, 284, 1133-1134.

Bond, G., Showers, W., Cheseby, M., Lotti, R., Almasi, P., deMenocal, P., Priore, P., Cullen, H., Hajdas, I. and Bonani, G., 1997. A pervasive Millennial-scale cycle in North Atlantic Holocene and glacial climates. Science, 278, 1257-1266.

Boenzi, F. and Palmentola, G., 1997. Glacial features and snow-line trends during the last glacial age in the Southern Apennines (Italy) and on Albanian and Greek mountains. Zeitschrift für Geomorphologie, 41, 21-29.

Cacho, I., Grimalt, J.O., Canals, M., Sbaffi, L., Shackleton, N.J., Schönfeld, J. and Zahn, R., 2001. Variability of the western Mediterranean Sea surface temperature during the last 25,000 years and its connection with the Northern Hemisphere climatic changes. Paleoceanography, 16, 40-52.

Cacho, I., Grimalt, J.O. and Canals, M., 2002. Response of the western Mediterranean Sea to rapid climatic variability during the last 50,000 years: a molecular biomarker approach. Journal of Marine Systems, 33-34, 253-272.

Cassou, C., Terray, L., Hurrell, J.W. and Deser, C., 2004. North Atlantic Winter Climate Regimes: Spatial asymmetry, stationarity with time, and oceanic forcing. Journal of Climate, 17, 1055-1068.

COHMAP Members, 1988. Climate changes of the last 18,000 years: Observations and model simulations. Science, 241, 1043-1052.

Dunai, T., 2000. Scaling factors for production rates of in situ produced cosmogenic nuclides: a critical evaluation. Earth and Planetary Science Letters, 176, 157-169.

Florineth, D. and Schlüchter, C., 1998. Reconstruction the Last Glacial Maximum (WUERMIAN) ice surface geometry and flowlines of the Central Swiss Alps. Eclogae Geologicae Helvetiae, 91, 391-407.

Florineth, D. and Schlüchter, C., 2000. Alpine evidence for atmospheric circulation patterns in Europe during the Last Glacial Maximum. Quaterary Research, 54, 295-308.

García-Ruiz, J.M., Valero-Garcés, B.L., Martí-Bono, C. and González-Sampériz, P., 2003. Asynchroneity of maximum glacier advances in the central Spanish Pyrenees. Journal of Quaternary Sciences, 18, 61-72.

Giraudi, C. and Frezzotti, M., 1997. Late Pleistocene Glacial Events in the Central Apennines, Italy. Quaternary Research, 48, 280-290.

Giraudi, C., 2004. The Apennine glaciations in Italy. In: J. Ehlers and P.L. Gibbard (eds.), Quaternary Glaciations – Extent and chronology. Developments in Quaternary Sciences, 2, pp. 215-223.

Harrison, S., Yu, G. and Tarasov, P.E., 1996. Late Quaternary lake-level record from northern Eurasia. Quaternary Research, 45, 138-159.

Hayes, A., Kucera, M., Kallel, N., Sbaffi, L. and Rohling, E.J., 2005. Glacial Mediterranean sea surface temperatures based on planktonic foraminiferal assemblages. Quaternary Science Reviews, 24, 999-1016.

Hughes, P.D., 2007. Recent behaviour of the Debeli Namet glacier, Durmitor, Montenegro. Earth Surface Processes and Landforms, 32, 1593-1602.

Hughes, P.D. and Woodward, J.C., 2008. Timing of glaciation in the Mediterranean mountains during the last cold stage. Journal of Quaternary Science, 23, 575-588.

Hughes, P.D., Woodward, J.C. and Gibbard, P.L., 2007. Middle Pleistocene cold stage climates in the Mediterranean: New evidence from the glacial record. Earth and Planetary Science Letters, 253, 50-56.

Jacobeit, J., Jönsson, P., Bärring, L., Beck, C. and Ekström, M., 2001. Zonal indices for Europe 1780-1995 and running correlations with temperature. Climatic Change, 48, 219-241.

Jacobshagen, V., Dürr, S., Kockel, F., Makris, J., Meyer, W., Röwer, P., Schröder, B., Seidel, E., Wachendorf, H., Dornsiepen, U., Giese, P. and Wallbrecher, E., 1986. Geologie von Griechenland. Beiträge zur Regionalen Geologie der Erde, 19, Borntraeger, Berlin-Stuttgart, 363 pp.

Jost, A., Lunt, D., Kageyama, M., Abe-Ouchi, A., Peyron, O., Valdes, PJ. and Ramstein, G., 2005. High-resolution simulations of the last glacial maximum climate over Europe: a solution to discrepancies with continental palaeoclimatic reconstructions? Climate Dynamics, 24, 577-590.

Kageyama, M., Lâıne A. and Abe-Ouchi, A., Braconnot, P., Cortijo, E. , Crucifix, M., de Vernal, A., Guiot, J., Hewitt, C.D., Kitoh, A., Marti, O., Ohgaito, R., Otto-Bliesner, B., Peltier, W.R., Rosell-Mele, A., Vettoretti, G., Weber, S.L. and MARGO Project Members, 2006. Last Glacial Maximum temperatures over the North Atlantic, Europe and western Siberia: a comparison between PMIP models, MARGO sea-surface temperatures and pollen-based reconstructions, Quaternary Science Reviews, 25, 82-2102.

Kohl, C.P. and Nishiizumi, K., 1992. Chemical isolation of quartz for measurement of in-situ-produced cosmogenic nuclides. Geochiminca and Cosmochimica Acta, 56, 3583-3587.

Kuhlemann, J., Van der Borg, K., Bons, P.D., Danišík, M. and Frisch, W., 2007. Erosion rates on subalpine palaeosurfaces in the western Mediterranean by in-situ ^{10}Be concentrations in granites: implications for surface processes and long-term landscape evolution in Corsica (France). International Journal of Earth Sciences, 97, 549-564.

Kuhlemann, J., Krumrei, I., Rohling E., Kubik, P., Ivy-Ochs S. and Kucera, M., 2008. Regional synthesis of Mediterranean atmospheric circulation during the Last Glacial Maximum. Science, 321, 1338-1340.

Kuhlemann, J., Gachev, E., Alexander Gikov, A., and Nedkov, S., in press 2009. Glacial extent in the Rila mountains (Bulgaria) as part of an environmental reconstruction of the Mediterranean during the Last Glacial Maximum (LGM). Proceedings of the Academy of Sciences of Bulgaria.

Larrassoana, J., Roberts, A.P., Rohling, E.J., Winklhofer, M. and Wehausen, R., 2003. Three million years of monsoon variability over the northern Sahara. Climate Dynamics, 21, 689-698.

Luterbacher, J. and 48 coauthors, 2005. Mediterranean climate variability over the last centuries: A review. In: P. Lionello, R. Malanotte-Rizzoli and R. Boscolo (eds.), The Mediterranean Climate: an overview of the main characteristics and issues, Elsevier, Amsterdam, pp. 27-148.

Marjanac, L. and Marjanac, T., 2004. Glacial history of the Croatian Adriatic and Coastal Dinarides. In: J. Ehlers and P.L. Gibbard (eds.), Quaternary Glaciations – Extent and Chronology. Part I: Europe. Elsevier, Amsterdam , pp. 19-26.

Menković, L., Marković, M., Čupković, T., Pavlović, R., Trivić, B. and Banjac, N., 2004. Glacial morphology of Serbia Yugoslavia, with comments on the Pleistocene glaciation of Montenegro, Macedonia and Albania. In: J. Ehlers and P.L. Gibbard. (eds), Quaternary Glaciations - Extent and chronology, Developments in Quaternary Sciences, 2, pp. 379-384.

Meland, M., Jansen, E. and Elderfield, H., 2005. Constraints on SST estimates for the northern North Atlantic/Nordic Seas during the LGM. Quaternary Science Reviews, 2, 835-852.

Messerli, B., 1967. Die eiszeitliche und gegenwärtige Vergletscherung im Mittelmeergebiet, Geographica Helvetica, 22, 105-228.

Milivojević, M., Menković, L., and Ćalić, J, 2008. Pleistocene glacial relief of the central part of Mt. Prokletije (Albanian Alps). Quaternary International, 190, 112-122.

Ocokoljić, M., Jovanović, V., Radovanović, M. and Vemić, M., 1994. Vodni resursi i režim voda šarplaninskih župa Gore, Opolja i Sredske (Water resources and water regime in the Sar-planina counties Gora, Opolje and Sredska; in Serbian). Special issues of the Geographical Institute “Jovan Cvijić” SANU, Belgrade, 40/1, 183-212.

Mountrakis, D., Kilias, A., Pavlides, S., Patras, D., and Spyropoulos, N., 1987. Structural geology of the Internal Hellenides and their role to the geotectonic evolution of the Eastern Mediterranean. Acta Naturalia de "L'Ateneo Parmense", 23/4, 147-161.

Pérez Alberti, A., Valcárel Díaz, M. and Blanco Chao, R., 2004. Pleistocene glaciation in Spain. In: J. Ehlers and P.L. Gibbard (eds.) Quaternary Glaciations – Extent and Chronology, Part I: Europe, Elsevier, pp. 389-394.

Pigati, J. and Lifton, N., 2004. Geomagnetic effects on time-integrated cosmogenic nuclide production with emphasis on in situ 14C and 10Be. Earth and Planetary Science Letters, 226, 193-205.

Porter, S.C., 2001. Snow line depression in the tropics during the last glaciation, Quaternary Science Reviews, 20, 1067-1091.

Reischmann, T., Kostopoulos, D.K., Loos, S., Anders, B., Avgerinas, A. and Sklavounos, S.A., 2001. Late Palaeozoic magmatism in the basement rocks southwest of Mt. Olympos, Central Pelagonian Zone, Greece: remnants of a Permo-Carboniferous magmatic arc. Bulletin of the Geological Society of Greece, 34, 985-993.

Reuther, A., Geiger, C., Urdea, P., Niller, H.-P. and Heine, K., 2004. Determining the glacial equilibrium line altitude (ELA) for the northern Retezat Mountains, Southern Carpathians and resulting paleoclimatic implications for the last glacial cycle. Analele Universităţii de Vest din Timişoara, Geografie, 14, 11-34.

Reuther, A., Urdea, P., Geiger, C., Ivy-Ochs, S., Niller, H.-P., Kubik, P. and Heine, K., 2007. Late Pleistocene glacial chronology of the Pietrele valley, Retezat Mountains, Southern Carpathians constrained by 10Be exposure ages and pedological investigations. Quaternary International, 164, 151-169.

Rohling, EJ., Hayes, A., Kroon, D., De Rijk S. and Zachariasse, WJ., 1998. Abrupt cold spells in the NW Mediterranean. Palaeoceanography, 13, 316-322.

Severinghaus, J.P. and Brook, E.J., 1999. Abrupt Climate Change at the End of the Last Glacial Period Inferred from Trapped Air in Polar Ice. Science, 286, 930-934.

Shackleton, N.J., Fairbanks, R.G, Chiu, T.C. and Parrenin, F., 2004. Absolute calibration of the Greenland time scale: implications for Antarctic time scales and for Δ^{14}C. Quaternary Science Reviews, 23, 1513-1522.

Solomon, S., Qin, D., Manning, M., Alley, R.B., Berntsen, T., Bindoff, N.L., Chen, Z., Chidthaisong, A., Gregory, J.M., Hegerl, G.C., Heimann, M., Hewitson, B., Hoskins, B.J., Joos, F., Jouzel, G., Kattsov, V., Lohmann, U., Matsuno, T., Molina, M., Nicholls, N., Overpeck, J., Raga, V., Ramaswamy, J., Ren, J., Rusticucci, M., Somerville, R., Stocker, T.F., Whetton, P., Wood, R.A. and Wratt., D., 2007. Technical Summary. In: S. Solomon, D. Qin, M. Manning, Z. Chen, M. Marquis, K.B. Averyt, M. Tignor and H.L. Miller (eds.), Climate Change 2007: The Physical Science Basis. Contribution of Working Group I to the Fourth Assessment Report of the Intergovernmental Panel on Climate Change. Cambridge University Press, Cambridge, 1009 pp.

Svendsen, J.I. and 29 coauthors, 2004. Late Quaternary ice sheet history of northern Eurasia. Quaternary Science Reviews, 23, 1229-1271.

Urdea, P., 2004. The Pleistocene glaciation of the Romanian Carpathians. Quaternary Glaciations – Extent and chronology. In: J. Ehlers and P.L. Gibbard (eds.), Quaternary Glaciations – Extent and chronology. Developments in Quaternary Sciences, 2, 301-308.

van Husen, D., 1997. Würmian and late-glacial fluctuations in the Eastern Alps. In: C.M. Clapperton (ed.), Fluctuations of local glaciers 30-8 ka BP, Quaternary International, 38-39, 109-118.

von Blanckenburg, F., Hewawasam, T. and Kubik, P., 2004. Cosmogenic nuclide evidence for low weathering and denudation in the wet, tropical highlands of Sri Lanka. Journal of Geophysical Research, 109, doi: 10.1029/2003JF000049.

Woodward, J.C., Macklin, M.G. and Smith, G.R., 2004. Pleistocene glaciation in the mountains of Greece. In: J. Ehlers and P.L. Gibbard (eds.), Quaternary Glaciations – Extent and chronology. Developments Quaternary Sciences, 2, 155-173.

Xoplaki, E., Maheras, P. and Luterbacher, J., 2001. Variability of climate in meridional Balkans during the periods 1675-1715 and 1780-1830 and its impact on human life. Climate Change, 48, 581-615.

Received: 9. March 2009
Accepted: 20. May 2009

Joachim KUHLEMANN[1)2)*)], Milovan MILIVOJEVIĆ[3)], Ingrid KRUMREI[2)] & Peter W. KUBIK[4)]

[1)] Swiss Nuclear Safety Inspectorate ENSI, CH-5232 Villigen-ENSI, Switzerland.

[2)] Institute for Geosciences, University of Tübingen, D-72076 Tübingen, Sigwartstr. 10, Germany.

[3)] Geographical Institute ''Jovan Cvijić'', Serbian Academy of Sciences and Arts, Belgrade, Serbia.

[4)] Laboratory of Ion Beam Physics, ETH Zurich, CH-8093 Zurich, Switzerland.

[*)] Corresponding author, kuj@ensi.ch